Thermal Infrared Emissivity Dependence on Soil Moisture in Field Conditions

Juan M. Sánchez, Andrew N. French, *Member, IEEE*, Maria Mira, Douglas J. Hunsaker, Kelly R. Thorp, Enric Valor, and Vicente Caselles

***Abstract*—An accurate estimate of land surface temperature, which is a key parameter in surface energy balance models, requires knowledge of surface emissivity. Emissivity dependence on soil water content has been already reported and modeled under controlled conditions at the laboratory. This paper completes and extends that previous work by providing emissivity measurements under field conditions without elimination of impurities, local heterogeneities, or soil cracks appearing in the drying process. The multispectral radiometer CE312-2, with five narrow bands and a broad band in the 8–13-μm range, was used, and surface emissivity values were determined through a temperature–emissivity separation algorithm. A bare soil plot of $10 \times 17\ \mathrm{m}^2$ was selected for this study in the framework of a camelina 2010 experiment. This experiment was carried out during March and April 2010 at The University of Arizona Maricopa Agricultural Center in central Arizona, USA. The soil plot was flood irrigated every two to three days and left to dry. Field emissivity measurements were collected under cloud-free skies, around noon, for different values of soil water content. Soil samples were collected to estimate the soil moisture (SM) using the gravimetric method. An overall increase of emissivity with SM was obtained in all channels. However, when wetted soils subsequently dried, the final minimum emissivity was greater than the initial minimum emissivity. This hysteresis could be due to cavity effects produced by soil cracks not originally present. Thus, the deterioration of soil surface tends to reduce the emissivity spectral contrast. Soil-specific and general relationships obtained by Mira *et al.* were tested and compared with the field measurements. Field emissivities agree within 2% with the modeled values for all bands under noncracked surface conditions, whereas differences reach 5% in the 8–9-μm range when cracks are present.**

***Index Terms*—Remote sensing, soil cracks, soil moisture (SM), temperature–emissivity separation (TES) method, thermal emissivity.**

Manuscript received December 10, 2010; revised February 25, 2011; accepted April 3, 2011. Date of publication May 27, 2011; date of current version October 28, 2011. This work was supported in part by the *Science and Innovation Ministry* (Projects CGL2007-64666_CLI and CGL2010-17577, cofinanced by FEDER funds, *Juan de la Cierva* Research Contract of Dr. Sánchez, and FPU Research Grant of Dra. Mira) and in part by *Generalitat Valenciana* (Project PROMETEO/2009/086).

J. M. Sánchez is with the Department of Applied Physics, School of Industrial Engineering of Albacete (EIIAB), University of Castilla-La Mancha, 02071 Albacete, Spain (e-mail: juanmanuel.sanchez@uclm.es).

A. N. French, D. J. Hunsaker, and K. R. Thorp are with the U.S. Arid Land Agricultural Research Center, Agricultural Research Service, U.S. Department of Agriculture, Maricopa, AZ 85138 USA.

M. Mira, E. Valor, and V. Caselles are with the Department of Earth Physics and Thermodynamics, Faculty of Physics, University of Valencia, 46100 Burjassot, Spain.

Color versions of one or more of the figures in this paper are available online at http://ieeexplore.ieee.org.

Digital Object Identifier 10.1109/TGRS.2011.2142000

I. Introduction

An ACCURATE estimate of land surface temperature (LST), which is a key parameter in long-wave surface energy balance models, requires knowledge of land surface emissivity (LSE). Thermal infrared (TIR) remote sensing provides an ideal method for the derivation of LST and LSE with a variety of spatial and temporal resolutions, depending on the sensor used [2]–[4]. It is known that changes in surface soil moisture (SM) yield variations in surface emissivity that should be accounted for in order to improve LSE characterization in climate models and minimize errors in model-simulated LST and surface fluxes. However, studies analyzing the emissivity and SM dependence in the TIR domain are still scarce [5]–[9]. Mira *et al.* [1] provided the results of TIR emissivity variation with SM for a set of 14 soil samples of different textures. These authors showed a common increase of emissivity with SM, more apparent in the 8–9-μm range, while the 10–12-μm channels showed little variation with either soil type or SM. Mira *et al.* [1] obtained soil-specific and general approaches to model TIR emissivity and SM dependence from laboratory measurements using the two-lid variant of the Box method [10]. Before and during each series of emissivity measurements, the sample was mixed, and soil cracks appearing in the drying process were eliminated. Hulley *et al.* [11] carried out a laboratory experiment to investigate the temporal TIR emissivity variation of two water-saturated sand samples. These authors used an infrared spectrometer with an integrating sphere to measure the emissivity of the sand samples contained in small Petri dishes.

Field measurements may differ from the results obtained in laboratory due to a variety of factors that cannot be controlled outdoors. This study is the first check on the validity under field conditions of the relationships between TIR emissivity and SM previously obtained in [1] from controlled laboratory measurements.

Thus, the objective of this paper is to compare and analyze the TIR emissivity and SM dependence under unaltered field conditions with those predicted from laboratory conditions. Both soil-specific and general equations obtained in [1] were tested. With this aim, an experimental site in central Arizona containing a bare soil plot was chosen. Emissivity spectra were obtained from ground-based measurements carried out at the field with the multiband radiometer CIMEL Electronique model CE312-2.

This paper proceeds as follows. The experimental site and measurement techniques are detailed in Section II. Section III describes the results and discussion of the experiment. Finally, main conclusions are summarized in Section IV.

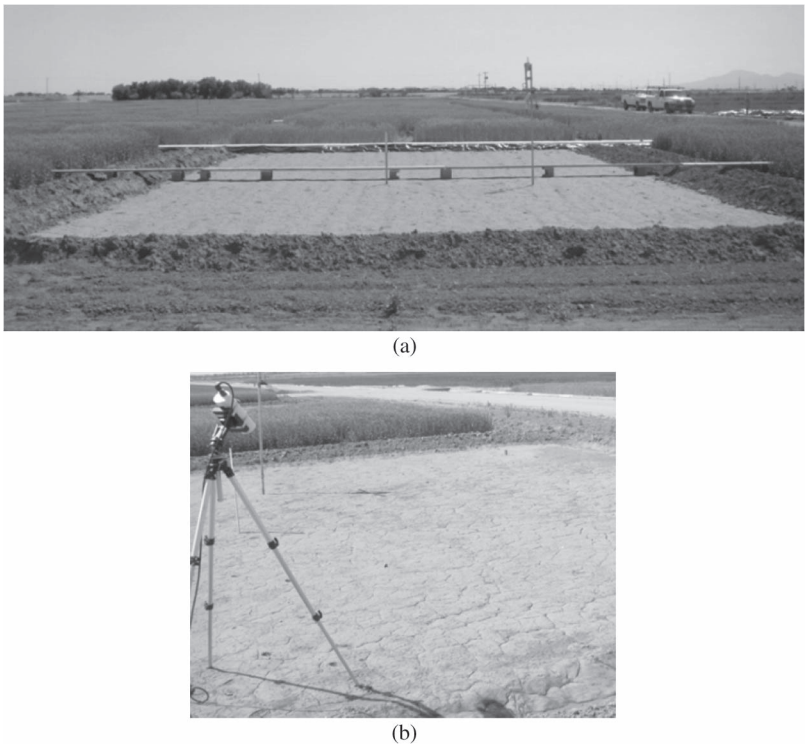

Fig. 1. Bare soil test plot at Maricopa. (a) View of plot from the north. (b) View from the southeast, showing typical experimental setup with the tripod-mounted thermal radiometer.

TABLE I
SOIL PROPERTIES, INCLUDING SOIL TEXTURE, TAXONOMIC CLASS, MINERAL AND ORGANIC COMPOSITION, BULK DENSITY, PERMANENT WILTING POINT (PWP), AND FIELD CAPACITY (FC)

Soil property	Value
Sand, %	65.1
Silt, %	14.7
Clay, %	20.2
Texture (USDA)	sandy clay loam
OM, %	0.43
$CaCO_3$, %	2.2
Quartz, %	58.4*
Bulk density, $g \cdot cm^{-3}$	1.48
PWP, m^3m^{-3}	0.121
FC, m^3m^{-3}	0.225

*Taken from sample LW52 in [1].

II. FIELD MEASUREMENTS

A. Experimental Setup

We selected a field area located at The University of Arizona Maricopa Agricultural Center (MAC) (33°04′ N, 111°58′ W; 361-m altitude) in central Arizona, USA. The 1.3-ha site (MAC field 111) was divided into 40 plots, 10 m × 17 m each. A flood irrigation system was set with water supplied by 152-mm gated pipe (Fig. 1). *Camelina sativa*, an oil seed crop, was planted in 38 of these plots, whereas 2 plots were maintained as bare soil to serve as a reference during the camelina 2010 experiment. One of the plots was flood irrigated every two to three days and left to dry, whereas the other was kept dry, with rain as its only water supply. Soil presented the same properties at both plots (shown in Table I). However, the structure of the wet soil surface layer deteriorated with time (Fig. 2), while the dry soil surface layer remained unaltered. This was the consequence of the periodic flooding and drying events that caused soil crack development. For this reason, we focused on the wet plot (Fig. 1). The measurements were carried out from the end of March to middle of May, 2010. Only cloud-free skies and calm-wind conditions were accepted. A total of 13 days were considered. Radiance measurements were taken with the high-precision multichannel TIR radiometer CIMEL Electronique CE312-2 [12]. The instrument has five narrow bands and one broadband in the spectral region between 8 and 13 μm. Table II shows the main technical specifications of the CIMEL instrument. The similarity between the CE312-2 bands and the Advanced Spaceborne Thermal Emission and Reflection radiometer (ASTER) TIR bands allows the application of the temperature–emissivity separation (TES) [13] algorithm for recovering surface emissivities from the ground-based measurements with no need to modify the calibration curve used by the TES algorithm. Table II also shows the specifications for a predecessor instrument, i.e., the CE312-1, which was used in [1] for developing emissivity–SM formulations. Note that the mismatch between the spectral ranges of the channels of the two CIMEL radiometers, namely, CE312-1 and CE312-2, may yield some minor differences in the emissivity results, but the overall findings of this paper will remain unaltered. A series of field emissivity measurements was collected in each soil plot for different values of soil water content.

B. SM Measurements

The gravimetric method was chosen for measuring the SM since this is the most accurate technique. This is a destructive

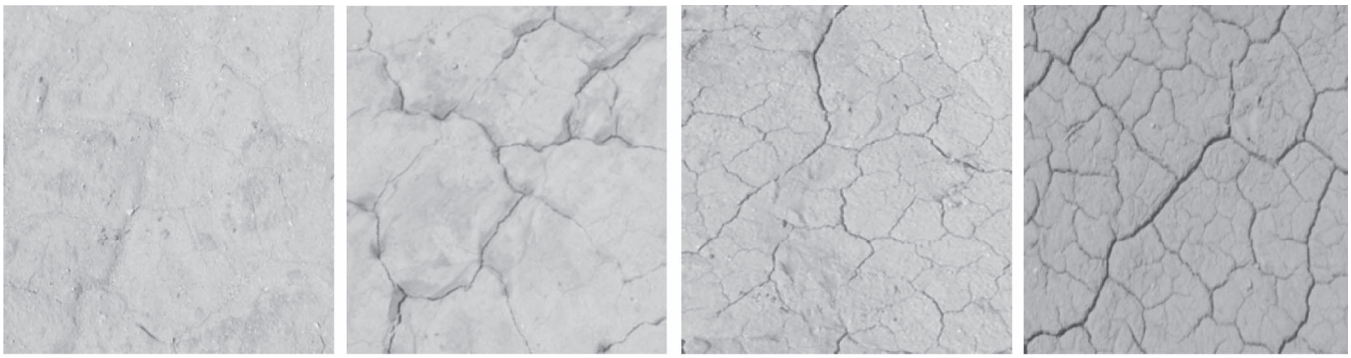

Fig. 2. Close-up view of the soil surface at different stages. Each image covers an area approximately 60 cm by 60 cm. Four stages are illustrated: (a) No flood applied, (b) after the first flood, with an average crack density of 2.9% ± 0.6%, (c) after five floods, with an average crack density of 4.0% ± 0.5%, and (d) after ten floods, with an average crack density of 4.9% ± 0.5%.

TABLE II
TECHNICAL SPECIFICATIONS OF THE THERMAL RADIOMETERS CIMEL ELECTRONIQUE CE312-1 AND CE312-2, EFFECTIVE WAVELENGTHS (λ_{eff}), AND SPECTRAL RANGE ($\Delta\lambda$)

CE312-2 channel	λ_{eff} (μm)	$\Delta\lambda$ (μm)	CE312-1 channel	λ_{eff} (μm)	$\Delta\lambda$ (μm)
1	-	8.01 - 13.34	1	-	8.0 - 13.3
2	11.296	10.86 - 11.71	2	11.96	11.5 - 12.4
3	10.567	10.16 - 10.96	3	10.80	10.2 - 11.3
4	9.145	8.95 - 9.34			
5	8.676	8.49 - 8.86	4	8.82	8.3 - 9.3
6	8.420	8.25 - 8.60			

method based on the immediate determination of soil water content [14]. In order to consider the SM variations caused by vapor exchange with the air above the sample, concurrent to the emissivity measurements, we took four soil samples of 10 to 30 g from the three first centimeters in depth. Their average value, together with their error, was considered as the SM measurement. Taking into account that the radiance observed by a TIR radiometer comes from the first few micrometers of the surface soil layer in direct contact with the atmosphere, we assumed that the surface vertical gradient in volumetric SM was not an important parameter for this study. The soil sample masses were measured with a balance with an accuracy of 10^{-5} kg. Because of this high accuracy, the SM error was, in general, caused by the nonideal homogeneity of SM during the measurement process. Following the gravimetric method, the sample is weighed before and after a 24-h drying period in an oven at 105 °C. The ratio of the mass of water present to the dry weight of the soil sample constitutes the gravimetric SM. Here, SM is expressed as the ratio of the volume of water present to the total volume of the wet soil sample. This volumetric SM can be obtained from gravimetric SM by considering the measured bulk density of the sample.

C. TES Algorithm

The TES algorithm was originally developed to produce the standard products of surface temperature and TIR emissivities from the ASTER data. Here, a variant was used for ground-based measurements. The algorithm is based on an empirical relationship between the range of emissivities for a set of TIR channels and their minimum value. It needs multispectral measurements but does not require either multitemporal or multidirectional observations. For a multispectral TIR sensor with n channels, there are $n+1$ unknowns (n spectral emissivities plus one LST) but only n measurements, so additional information is required.

In TES, the ill-posed problem is addressed by combining three prior approaches to obtain an improved accuracy for the estimates of emissivity absolute values. The first of these is the normalized emissivity procedure (NEM), which uses an initial value of emissivity (typically, $\varepsilon = 0.95$ for bare soils) to obtain temperature values for each channel. The maximum temperature calculated is considered as the initial value of LST, which, in turn, is used to obtain revised estimates of the emissivities for every channel. The second approach is a ratio procedure, which obtains relative emissivities, by ratioing NEM emissivities to their average value. The third approach is the maximum–minimum difference (MMD) procedure, which uses an empirical relationship between the minimum emissivity $(\varepsilon_{\min})$ and the spectral contrast

$$\varepsilon_{\min} = 0.985 - 0.738\, MMD^{0.856}. \tag{1}$$

Equation (1) is derived from the laboratory spectral measurements of soil, vegetation, and water and is appropriate for agricultural areas [15].

Using the CE312-2, four measurements of the at-surface radiance L_i^{surf} (where i is a channel index) per channel were made over each location. Each channel measurement requires 20 s, and thus, measurements for all channels require 2 min. Eight data sets of L_i^{surf} were measured over each site so that multiple emissivity spectra can be retrieved for comparisons. Close in time, a series of radiometric measurements of the sky was made to estimate the downwelling atmospheric radiance L_i^{sky}. Since only cloudless sky conditions were considered and the area was free of trees or buildings, the effect of errors in L_i^{sky} was small.

The TES algorithm was then applied, and spectral emissivities were calculated using a simplified expression of the

radiative transfer equation

$$\varepsilon_i = \frac{L_i^{\text{surf}} - L_i^{\text{sky}}}{B_i(T) - L_i^{\text{sky}}} \tag{2}$$

where B is blackbody spectral radiance from Planck's law.

Reference [16] showed in a sensitivity analysis that the effect of the radiometric error of the CIMEL on the TES results is less than 1% and that a systematic error of about 2% is obtained for high-contrast surfaces. These authors also studied the influence of the nonsimultaneity of the measurements on the emissivity values retrieved by the TES method. Differences less than 0.2% were obtained for all channels, which were less than the standard deviation of our TES measurements. We can then conclude that the nonsimultaneity of the TES measurements did not affect the accuracy of emissivity retrievals in our experiment.

III. Results and Discussion

A. TIR Emissivity and SM Dependence

Mean emissivities, along with their standard deviations, from the field measurements are plotted versus the volumetric SM in Fig. 3. As expected, there is a common increase of TIR emissivities with SM. This increase is larger than the standard uncertainty of the measurements (Table III). The highest variation of emissivity with SM, reaching 5%, is observed in channels 4 and 5 (8.49–9.34 μm). This is due to the strong absorbing features of water in the region of the quartz reststrahlen bands (7.7 and 9.7 μm) [12]. References [1] and [18] showed that the emissivity of a variety of different soils varies from 1.7% to 16% with increasing SM content in these bands. The same maximum variation of 5% was obtained in [1] for a soil sample (labeled as LW52) that is very similar in composition to the one studied here. However, the emissivity variation obtained in our study site is lower than that shown in [1] for larger wavelengths. The presence of carbonates in our sample (see Table I) can explain this different behavior since carbonate spectrum shows a weak absorption feature centered near 11.2 μm [17].

Note that emissivity errors are larger than average at SM values around 0.20 $\text{m}^3 \cdot \text{m}^{-3}$. These are due to the inhomogeneity of the soil surface under these SM conditions, which was characterized by dark and light patches within the soil plot.

B. Crack Density Effect on Thermal Emissivities

Data were grouped into three subsets corresponding to different soil deterioration degree, drying time, and number of irrigation events. The drying process of the sample took two to four days, depending on the atmospheric conditions. At an early stage, the soil structure was smooth with no cracks [Fig. 2(a)]. After the first flooding, some cracks appeared [Fig. 2(b)]. At this stage, the soil surface was deteriorating, where cracking density, depth, and width all increased. Fig. 2(c) and (d) shows the soil surface state after five and ten floods, respectively. The value of the crack density (estimated by digital image processing) was used to quantify the degree of soil surface deterioration of the different subsets. The assigned error includes the effect of the spatial and temporal inhomogeneities of the measurements.

It was generally observed that emissivity increased with SM, particularly when soil cracking was minimal. The cavity effect produced by the presence of cracks in the soil tended to increase the TIR emissivity values [19], particularly at lower wavelengths (Fig. 3). Similar findings were observed when emissivities were related to cracking density for a fixed SM content of 0.09 $\text{m}^3 \cdot \text{m}^{-3}$ (Fig. 4). It is evident that the emissivity spectral contrast increases when the crack density is lower, particularly when considering emissivities before the first flooding. In this case, when no cracks were present, emissivity values were the lowest, particularly at shorter wavelengths, with the consequent increase of the spectral contrast. We may then conclude that the behavior of the TIR emissivity and SM dependence is dramatically influenced by the presence of soil surface cracks, whereas the effect of the increase in crack density was much less important, with deviations mostly less than experimental errors.

C. Comparison With Modeled Values

Reference [1] determined a logarithmic dependence of TIR emissivity on SM following the equation

$$\varepsilon_i = a_i + b_i\theta_v + c_i \ln(\theta_v) \tag{3}$$

where θ_v is the volumetric SM and a_i, b_i, and c_i are the coefficients for channel i of the CIMEL model CE312-1. Specific coefficients were given for the 14 different soil types analyzed. With the aim of improving the applicability of (3), general coefficients (GCs) were also estimated [1]. In this paper, we tested both soil-specific coefficient (SSC) and GC relationships. Furthermore, predictability can be improved by including other parameters that influence the emissivity spectrum, such as organic matter (OM), quartz (Q), and carbonate (C) contents [1]

$$\varepsilon_i = a_i + b_i\theta_v + c_i \ln(\theta_v) + d_i OM + e_i OM^2 + f_i Q + g_i C \tag{4}$$

where a to g are empirical coefficients for each spectral channel i, and the OM, Q, and C contents are given in percentage. One the one hand, the Q content increases the reflectance of the material and decreases the emissivity between 7.7 and 9.7 μm, due to the weak absorption feature of the quartz reststrahlen bands. On the other hand, the OM content, which is highly absorbing in the 8–14-μm region, reduces the apparent spectral contrast of these quartz reststrahlen bands [20].

Figs. 3 and 4 show the results of applying (3) and (4) to the different SM values reached in our experiment. Note that the coefficients in (3) and (4) were obtained for the four channels of the CIMEL CE312-1, while the six-channel CIMEL CE312-2 was used in this study for the field measurements. Table II shows the similitude of channels 1, 2, and 3 between the two radiometers, whereas the closest channel of CE312-2 to channel 4 of CE312-1 is channel number 5. Coefficients corresponding to the sample LW52 in [1] were considered in this study, given the similarity between their soil texture.

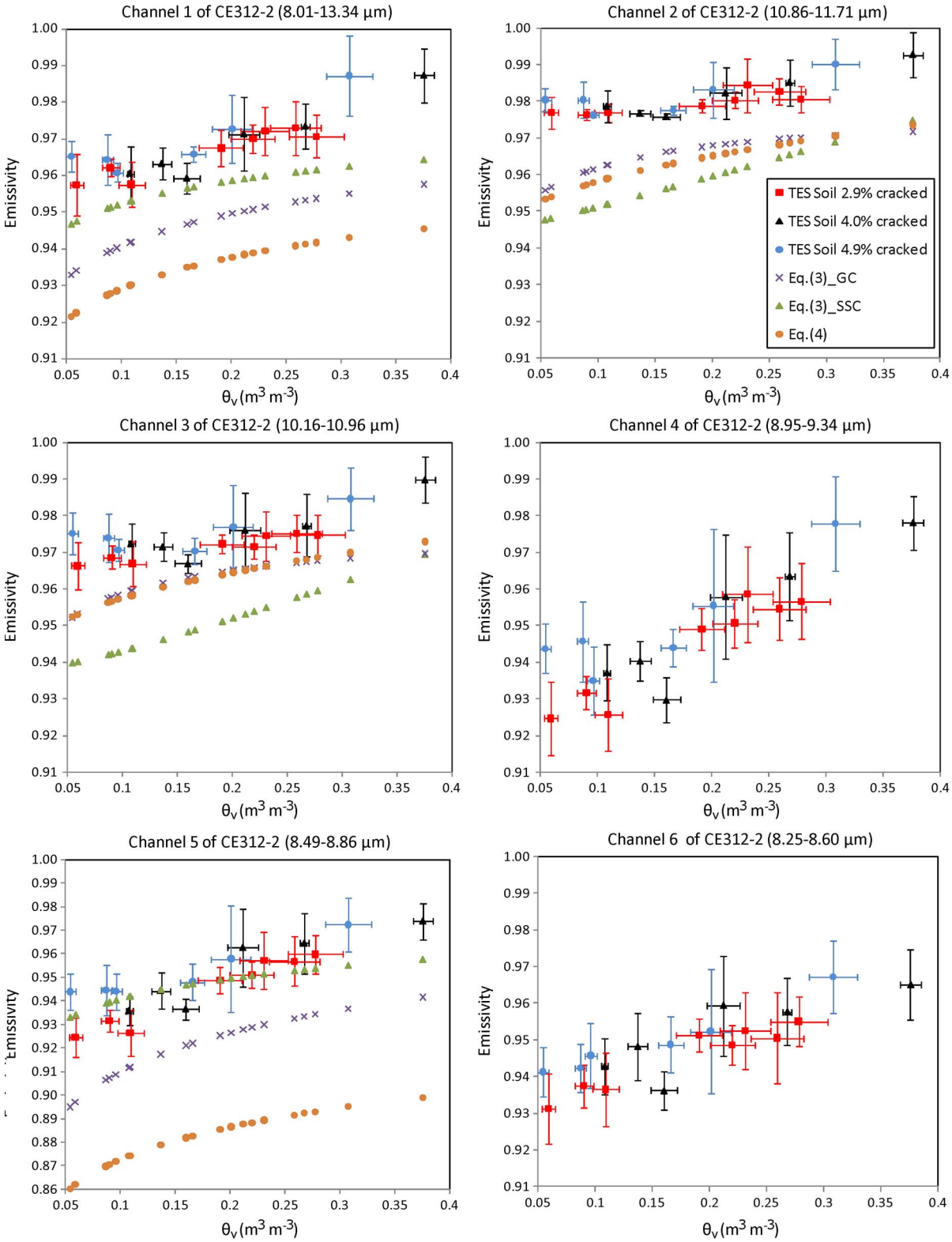

Fig. 3. Soil emissivity versus SM. Measured and modeled emissivities are shown for each of the six CIMEL 312-2 channels for SM ranging between 0.05 and 0.40 $m^3 \cdot m^{-3}$. Measurements are shown for three surface-cracking densities: 2.9%, 4.0%, and 4.9%. Modeling results are shown for the (3) and (4) approaches. GC and SSC refer to general coefficients and soil-specific coefficients, respectively.

Moreover, note that some soil properties, such as the C content, may have changed slightly during the experiment.

The plots in Fig. 3 and the emissivity variation values listed in Table III show that the GC from (3) was superior to the SSC from (3) when modeling the SM-emissivity variation for all bands except narrow band 3. Also, the underestimation of the absolute emissivity values was more evident using the specific coefficients in channels 2 and 3. However, for channel 5, the GC

TABLE III
EMISSIVITY RANGE (i.e., DIFFERENCE BETWEEN THE HIGHEST AND THE LOWEST EMISSIVITY VALUE) WITHIN THE WHOLE SM RANGE OBSERVED ($\Delta\varepsilon_i$) AND ITS ERROR ($\delta(\Delta\varepsilon_i)$), AND THE AVERAGE OF STANDARD UNCERTAINTY OF THE MEASUREMENTS ($\delta\varepsilon_i$), IN THE SIX SPECTRAL CHANNELS OF CE312-2. ALSO, $\Delta\varepsilon_i$ IS MODELED USING (3) AND (4)

CE312-2 channel	$\Delta\varepsilon_i \pm \delta(\Delta\varepsilon_i)$	$\overline{\delta\varepsilon_i}$	CE312-1 channel	$\Delta\varepsilon_i$ SSC from Eq (3)	$\Delta\varepsilon_i$ GC from Eq (3)	$\Delta\varepsilon_i$ from Eq (4)
1	0.030±0.011	0.004	1	0.017	0.025	0.024
2	0.017±0.006	0.006	2	0.027	0.016	0.020
3	0.024±0.008	0.006	3	0.030	0.017	0.021
4	0.053±0.012	0.009				
5	0.049±0.012	0.009	4	0.025	0.047	0.039
6	0.036±0.014	0.009				

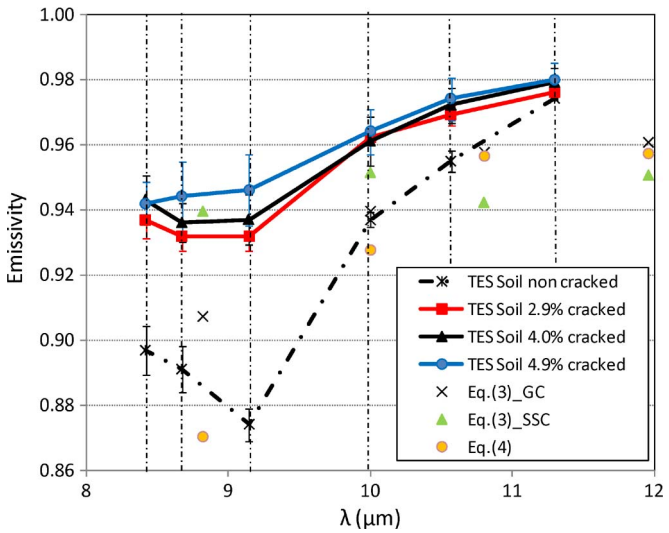

Fig. 4. Emissivity spectra for differing surface-cracking densities at uniform SM (0.09 $m^3 \cdot m^{-3}$). The lines denote the TES-based measurements, while the symbols denote the modeling results from the (3) and (4) approaches.

from (3) shows a significant systematic underestimation. When introducing OM, C, and Q content information through (4), no significant difference in terms of SM-emissivity variation was observed when compared to the results from (3) using the GCs. Moreover, similar absolute emissivity values were reproduced by (4) and GC from (3) for channels 2 and 3, while significant lower values were obtained for channel 5. The reason is the low OM content of this soil, which increases the apparent spectral contrast of the quartz reststrahlen bands [20].

Fig. 4 compares the emissivity measured in the field under uniform SM conditions ($\sim 0.09\ m^3 \cdot m^{-3}$) with those modeled by (3) and (4). The results from applying SSC (3) show low spectral contrast, closer to the cracked samples than to the noncracked ones. This finding is contrary to what was expected for laboratory measurements: Homogeneous nondeteriorated soil samples were anticipated to have relatively high spectral contrast. This can be justified again by the higher value of OM of the sample used to extract those SSC in [1] compared to the OM content of the present soil sample, which tends to reduce the spectral contrast of the modeled emissivity values, as mentioned before.

The emissivity values, along with their standard deviations, from the measurements over the noncracked sample, are summarized in Table IV. The results from (3) and (4) are also included in Table IV. Note that the differences between the modeled and the measured values were lower when using (4) together with the OM, Q, and C content information. This decrease was particularly significant for channel 5, supporting the significance of the OM data in the modeled emissivity values. Similar differences were also obtained when modeling emissivity using GC from (3). Overall, the differences between the predicted and the measured emissivity values were less than 2% for all channels when using GC from (3) and (4) together with ancillary soil composition information. These results are an improvement over those obtained in [16]. In that study, agreement was less than 3% for the longer wavelength bands at 10.6–, 11.3–, and 8–13 μm, while the Box method results in overestimates that ranged between 2% and 7% for bands in the 8–9-μm range.

IV. SUMMARY AND CONCLUSION

The TIR emissivities of a particular soil were measured under real field conditions for a wide range of SM contents in order to confirm the emissivity–SM dependence previously observed in laboratory measurements and modeled in [1]. TIR emissivities were determined using a ground-adapted version of the TES algorithm, together with the high-precision multichannel TIR radiometer CIMEL Electronique CE312-2. Soil water contents were determined by using the gravimetric method.

The expected increase of emissivity with SM was confirmed in this paper from the TES field measurements. Also, the more apparent increase in the 8–9-μm range, due to the presence of Q, and the little variation in the 10–12 μm were maintained in these field measurements.

A new finding in this paper is that the influence of SM on TIR emissivity also depends upon the conditions of the soil surface, i.e., a different behavior of the increase of emissivity with SM is observed, depending on whether the surface is cracked or not. Results have shown that the cavity effect produced by the presence of cracks in the soil surface tends to increase the emissivity values under similar SM contents. Moreover, this change in the behavior was more abrupt after the first flood. This tendency continued, but more moderately, when the crack density, together with their depth and width, increases as a result of the progressive deterioration of the soil surface as a consequence of the floods.

The relationships inferred in [1] under laboratory conditions were tested using the present data set. Good agreement was

TABLE IV
MEASURED AND MODELED FIELD EMISSIVITIES FOR NONCRACKED SOILS. LISTED FOR EACH CIMEL CHANNEL ARE THE MEAN SPECTRAL EMISSIVITIES (ε), STANDARD ERRORS ($\delta(\varepsilon)$), SSC FROM (3) MODELED EMISSIVITIES, MEASURED VERSUS SSC FROM (3) MODELED DIFFERENCES, GC FROM (3) MODELED EMISSIVITIES, MEASURED VERSUS GC FROM (3) MODELED DIFFERENCES, (4) MODELED EMISSIVITIES, AND MEASURED VERSUS (4) MODELED EMISSIVITIES

CIMEL channel	$\varepsilon_i \pm \delta(\varepsilon_i)$ (non-cracked)	ε_i SSC from Eq (3)	Diff. ε_i	ε_i GC from Eq (3)	Diff. ε_i	ε_i from Eq (4)	Diff. ε_i
1	0.937±0.002	0.951	0.014	0.939	0.002	0.928	-0.009
2	0.9740±0.0002	0.951	-0.023	0.961	-0.013	0.957	-0.017
3	0.955±0.003	0.942	-0.013	0.958	0.003	0.957	0.002
4	0.874±0.005						
5	0.891±0.007	0.939	0.042	0.907	0.016	0.870	-0.021
6	0.897±0.008						
RMSE			*0.026*		*0.010*		*0.014*

generally observed between the emissivity variations measured and modeled using (3) with the GCs and (4). The discrepancy observed in the 8.7-μm channel between the measured and the modeled value using (3) adapted to the texture of this soil (specific coefficients) can be explained by the lower OM content of the soil sample analyzed in this paper in comparison with sample LW52 from [1]. For the same reason, the SSC from (3) reproduced a flat spectrum, whereas the GC from (3) and (4) results succeeded in capturing the observed spectral contrast over the noncracked soil surface with differences between the predicted and the measured emissivity values less than 2% for all channels and less than 1% (sometimes less than 0.5%) for channel 1 (broadband) and channel 3 (10.567 μm), respectively.

Even though the emissivity–SM dependence is investigated here on a limited area and a short time, the results from this study under field conditions support those previously obtained at the laboratory. Further work is required to test whether LSE variations from multispectral thermal sensors (MODIS, ASTER, HyspIRI, etc.) over bare and semiarid areas might be better understood by introducing the emissivity–SM dependence as a new factor. The SM data from the Soil Moisture and Ocean Salinity sensor will be used for this aim.

ACKNOWLEDGMENT

The authors would like to thank the logistic support in operating and maintaining the camelina 2010 experimental site of the Arid-Land Agricultural Research Center (ALARC), and The University of Arizona Maricopa Agricultural Center. During this study, Dr. Sánchez was with ALARC as a Visitor Researcher.

REFERENCES

[1] M. Mira, E. Valor, V. Caselles, E. Rubio, C. Coll, J. M. Galve, R. Niclòs, J. M. Sánchez, and R. Boluda, "Soil moisture effect on thermal infrared (8–13 μm) emissivity," *IEEE Trans. Geosci. Remote Sens.*, vol. 48, no. 5, pp. 2251–2260, May 2010.

[2] G. C. Hulley and S. Hook, "Generating consistent land surface temperature and emissivity products between ASTER and MODIS data for Earth science research," *IEEE Trans. Geosci. Remote Sens.*, vol. 49, no. 4, pp. 1304–1315, Apr. 2011. DOI: 10.1109/TGRS.2010.2063034.

[3] Y. Yu, J. P. Privette, and A. C. Pinheiro, "Evaluation of split window land surface temperature algorithms for generating climate data records," *IEEE Trans. Geosci. Remote Sens.*, vol. 46, no. 1, pp. 179–192, Jan. 2008.

[4] I. F. Trigo, L. F. Peres, C. C. DaCamara, and S. C. Freitas, "Thermal land surface emissivity retrieved from SEVIRI/Meteosat," *IEEE Trans. Geosci. Remote Sens.*, vol. 46, no. 2, pp. 307–314, Feb. 2008.

[5] M. Urai, T. Matsunaga, and T. Ishii, "Relationship between soil moisture content and thermal infrared emissivity of the sand sampled in Muus Desert, China," *Remote Sens. Soc. Jpn.*, vol. 17, no. 4, pp. 322–331, 1997.

[6] Q. Xiao, Q. H. Liu, W. Li, F. Chen, Q. Liu, and X. Z. Xin, "A field measurements method of spectral emissivity and research on the feature of soil thermal infrared emissivity," *J. Infrared Millim. Waves*, vol. 22, no. 5, pp. 373–378, 2003.

[7] K. Ogawa, T. Schmugge, and S. Rokugawa, "Estimating broadband emissivity of arid regions and its seasonal variations using thermal infrared remote sensing," *IEEE Trans. Geosci. Remote Sens.*, vol. 46, no. 2, pp. 334–343, Feb. 2008.

[8] K. Ogawa, T. J. Schmugge, and S. Rokugawa, "Observations of the dependence of the thermal infrared emissivity on soil moisture," *Geophys. Res. Abstr.*, vol. 8, p. 04 996, 2006.

[9] A. Lesaignoux, S. Fabre, X. Briottet, and A. Olioso, "Soil moisture impact on lab measured reflectance of bare soils in the optical domain [0.4–15 μm]," in *Proc. IEEE Int. Geosci. Remote Sens. Symp.*, 2009, vol. 3, pp. 3522–3525.

[10] E. Rubio, V. Caselles, and C. Badenas, "Emissivity measurements of several soils and vegetation types in the 8–14 μm wave band: Analysis of two field methods," *Remote Sens. Environ.*, vol. 59, no. 3, pp. 490–521, Mar. 1997.

[11] G. C. Hulley, S. J. Hook, and A. M. Baldridge, "Investigating the effects of soil moisture on thermal infrared land surface temperature and emissivity using satellite retrievals and laboratory measurements," *Remote Sens. Environ.*, vol. 114, no. 7, pp. 1480–1493, Jul. 2010.

[12] G. Brogniez, C. Pietras, M. Legrand, P. Dubuisson, and M. Haeffelin, "A high-accuracy multiwavelenght radiometer for *in situ* measurements in the thermal infrared. Part II: Behavior in field experiments," *J. Atmos. Ocean. Technol.*, vol. 20, no. 7, pp. 1023–1033, Jul. 2003.

[13] A. R. Gillespie, S. Rokugawa, T. Matsunaga, J. S. Cothern, S. Hook, and A. B. Kahle, "A temperature and emissivity separation algorithm for Advanced Spaceborne Thermal Emission and Reflection radiometer (ASTER) images," *IEEE Trans. Geosci. Remote Sens.*, vol. 36, no. 4, pp. 1113–1126, Jul. 1998.

[14] P. R. Day, *Methods of Soil Analysis, Part I. Physical and Mineralogical Properties, Including Statistics of Measurements and Sampling*. Madison, WI: Amer. Soc. Agronomy, 1965, pp. 545–567.

[15] J. C. Jiménez-Muñóz and J. A. Sobrino, "Emissitivity spectra obtained from field and laboratory measurements using the temperature and emissivity separation algorithm," *Appl. Opt.*, vol. 45, no. 27, pp. 7104–7109, Sep. 2006.

[16] M. Mira, T. J. Schmugge, E. Valor, V. Caselles, and C. Coll, "Comparison of thermal infrared emissivities retrieved with the two-lid box and the TES methods with laboratory spectra," *IEEE Trans. Geosci. Remote Sens.*, vol. 47, no. 4, pp. 1012–1021, Apr. 2009.

[17] L. C. Rowan and J. C. Mars, "Lithologic mapping in the Mountain Pass, California area using Advanced Spaceborne Thermal Emission and Reflection radiometer (ASTER) data," *Remote Sens. Environ.*, vol. 84, no. 3, pp. 350–366, Mar. 2003.

[18] M. Mira, E. Valor, R. Boluda, V. Caselles, and C. Coll, "Influence of soil water content on the thermal infrared emissivity of bare soils: Implication for land surface temperature determination," *J. Geophys. Res.*, vol. 112, p. F04 003, 2007. DOI: 10.1029/2007JF000749.

[19] E. Valor and V. Caselles, "Mapping land surface emissivity from NDVI: Application to European, African, and South American areas," *Remote Sens. Environ.*, vol. 57, no. 3, pp. 167–184, Sep. 1996.

[20] J. W. Salisbury and D. M. D'Aria, "Infrared (8–14 μm) remote sensing of soil particle size," *Remote Sens. Environ.*, vol. 42, no. 2, pp. 157–165, Nov. 1992.

Juan M. Sánchez received the B.Sc., M.Sc., and Ph.D. degrees in physics from the University of Valencia, Valencia, Spain, in 2003, 2005, and 2008, respectively.

He is currently a Postdoctoral Researcher with the Department of Applied Physics, School of Industrial Engineering of Albacete, University of Castilla-La Mancha, Albacete, Spain. He has published 20 papers in international journals, 3 book chapters and more than 30 conference papers. He has participated in more than ten national and international projects. His research interests focus on the thermal infrared remote sensing in general and the surface-energy-flux retrieval in particular.

Dr. Sánchez was the recipient of the Norbert Gerbier-MUMM International Award from the Executive Council of the World Meteorological Organization in 2010.

Andrew N. French (M'08) received the B.S. degree in geology and physics from Tufts University, Medford, MA, in 1976, the M.S. degree in geology from the University of Michigan, Ann Arbor, in 1978, and the B.S., M.S., and Ph.D. degrees in civil engineering from the University of Maryland, College Park, in 2001.

He is currently a Research Physical Scientist with the U.S. Arid Land Agricultural Research Center, Agricultural Research Service, U.S. Department of Agriculture, Maricopa, AZ. His current research is on the estimation of evapotranspiration using remote sensing with emphasis on multispectral thermal infrared remote sensing. He also works on the applications of remote sensing for the optimization of irrigation scheduling and detection of crop water stress.

Maria Mira was born in Ontinyent, Spain, in 1982. She received the B.Sc. (with first class honors), M.Sc., and Ph.D. degrees in physics from the University of Valencia, Burjassot, Spain, in 2005, 2007, and 2010, respectively.

She is currently a Researcher with the Department of Earth Physics and Thermodynamics, Faculty of Physics, University of Valencia. She was a visiting student at New Mexico State University, Las Cruces, from December 2007 to March 2008 and at the Institut National de la Recherche Agronomique, Bordeaux, France, from September 2009 to December 2009. Her research interest focuses on the physical processes of thermal infrared remote sensing, including the retrieval of surface emissivity from thermal infrared remotely sensed data supplied by the Moderate Resolution Imaging Spectroradiometer and the Advanced Spaceborne Thermal Emission and Reflection Radiometer sensors, as well as by field radiometers.

Douglas J. Hunsaker received the B.S. and M.S. degrees in agricultural engineering from Oregon State University, Corvallis, in 1982 and 1984, respectively, and the Ph.D. degree in agricultural and biosystems engineering from The University of Arizona, Tucson, in 1995.

He is currently an Agricultural Engineer with the U.S. Arid Land Agricultural Research Center, Agricultural Research Service, U.S. Department of Agriculture, Maricopa, AZ. His current research is on the estimation of crop evapotranspiration combining remote sensing and reference evapotranspiration methods. He also works on the applications of remote sensing for the optimization of irrigation scheduling and detection of crop water stress.

Kelly R. Thorp received the B.S. and M.S. degrees in agricultural engineering from the University of Illinois, Urbana, in 2000 and 2002, respectively, and the Ph.D. degree in agricultural engineering from Iowa State University, Ames, in 2006.

He is currently a Research Agricultural Engineer with the U.S. Arid Land Agricultural Research Center, Agricultural Research Service, U.S. Department of Agriculture, Maricopa, AZ. His current research is on the development of techniques to interface remote sensing with cropping-system simulation models and the application of these technologies to improve temporal and spatial management of water and nutrients in agricultural systems.

Enric Valor received the B.Sc., M.Sc., and Ph.D. degrees in physics from the University of Valencia, Burjassot, Spain, in 1992, 1994, and 1997, respectively.

He is currently an Associate Professor of earth physics with the Department of Earth Physics and Thermodynamics, Faculty of Physics, University of Valencia. He has published 35 papers in international journals and 45 conference papers. His research interest focuses on the physical processes of thermal infrared remote sensing, emissivity measurement and characterization, atmospheric and emissivity corrections, and temperature–emissivity separation algorithms.

Vicente Caselles received the B.Sc., M.Sc., and Ph.D. degrees in physics from the University of Valencia, Valencia, Spain, in 1980, 1981, and 1983, respectively.

He is currently a Professor of applied physics and the Head of the Thermal Remote Sensing Group, University of Valencia, Burjassot, Spain. He has an expertise of 32 years in the physical processes involved in both the temperature measurement and evapotranspiration using remote sensing techniques, which has been documented through 10 books, 20 doctoral theses, 100 papers in international journals, 60 conference papers, and 30 reports. He was collaborating with ESA as a Member of the Advisory Group for the Land-Surface Processes and Interactions Mission. He is currently the Manager of Human Resources and Researchers Mobility General Direction at the Spanish Ministry of Science and Innovation.

Dr. Caselles was the recipient of the Norbert Gerbier-MUMM International Award from the Executive Council of the World Meteorological Organization in 2010. He was the Chairman of the Spanish Remote Sensing Society.